Maintenance of embryonic auxin gradients for apical-basal patterning by PIN-FORMED-dependent auxin transport in Arabidopsis

Weijers, D.; Sauer, A.; Meurette, O.; Friml, J.; Ljung, K.; Sandberg, S.; ... ; Offringa, R.

The Plant Cell, Vol. 17, 2517–2526, September 2005, www.plantcell.org

Maintenance of Embryonic Auxin Distribution for Apical-Basal Patterning by PIN-FORMED–Dependent Auxin Transport in *Arabidopsis* [W]

Dolf Weijers,[a,b] Michael Sauer,[b] Olivier Meurette,[a] Jiří Friml,[b] Karin Ljung,[c] Göran Sandberg,[c] Paul Hooykaas,[a] and Remko Offringa[a,1]

[a] Developmental Genetics, Institute of Biology, Leiden University, Clusius Laboratory, 2333 AL Leiden, The Netherlands
[b] Developmental Genetics, Center for Molecular Biology of Plants, University of Tübingen, D-72076 Tübingen, Germany
[c] Umeå Plant Science Center, Department of Forest and Plant Physiology, Swedish University of Agricultural Sciences, SE 901 83 Umeå, Sweden

Molecular mechanisms of pattern formation in the plant embryo are not well understood. Recent molecular and cellular studies, in conjunction with earlier microsurgical, physiological, and genetic work, are now starting to define the outlines of a model where gradients of the signaling molecule auxin play a central role in embryo patterning. It is relatively clear how these gradients are established and interpreted, but how they are maintained is still unresolved. Here, we have studied the contributions of auxin biosynthesis, conjugation, and transport pathways to the maintenance of embryonic auxin gradients. Auxin homeostasis in the embryo was manipulated by region-specific conditional expression of indoleacetic acid-tryptophan monooxygenase or indoleacetic acid-lysine synthetase, bacterial enzymes for auxin biosynthesis or conjugation. Neither manipulation of auxin biosynthesis nor of auxin conjugation interfered with auxin gradients and patterning in the embryo. This result suggests a compensatory mechanism for buffering auxin gradients in the embryo. Chemical and genetic inhibition revealed that auxin transport activity, in particular that of the PIN-FORMED1 (PIN1) and PIN4 proteins, is a major factor in the maintenance of these gradients.

INTRODUCTION

Embryogenesis transforms the fertilized egg cell, the zygote, into a mature embryo that contains different organs built from many specialized cell types. The controlled specification of different cell types—pattern formation—ensures a species-specific body plan. Embryo pattern formation in the model dicotyledonous plant species *Arabidopsis thaliana* is characterized by nearly invariant cell divisions (Mansfield and Briarty, 1991; Jürgens and Mayer, 1994) that mark patterning events and stages and allow easy detection of defects in this process.

First, the zygote divides asymmetrically to yield a smaller apical cell that generates most of the embryo and a larger basal cell that generates a filamentous supporting structure, the suspensor. At the globular stage of embryo development, cells in the center of the proembryo elongate along the future shoot–root axis. Simultaneously, the uppermost suspensor cell (hypophysis) switches from extraembryonic to embryonic fate and contributes to the establishment of the root meristem. Later, localized cell division activity at the apical flanks of the globular embryo initiates the cotyledons and transforms the embryo into a heart shape. At this stage, all embryo organs have been initiated, and later steps involve elongation growth and maturation of the embryo.

Despite its fundamental importance in shaping the future plant, regulatory molecules and mechanisms in plant embryo pattern formation have been identified only recently. Through genetics, several genes required for normal embryo patterning have been defined. Elucidating the function of these genes has not led to a unified model for embryo development, but the activity of some of the encoded proteins implicates the plant signaling molecule auxin (Weijers and Jürgens, 2005).

Auxin is a central regulator in many processes during plant growth and development. An important aspect of auxin action is its directional transport through the plant (Friml, 2003). This polar auxin transport (PAT) is important for many auxin-regulated processes and requires the activity of polarly localized efflux regulators, represented by members of the PIN-FORMED family. PAT can be inhibited by naphthylphthalamic acid (NPA) and other drugs. Treatment of immature embryos with such PAT inhibitors leads to embryo patterning defects in several plant species (Schiavone and Cooke, 1987; Liu et al., 1993; Hadfi et al., 1998; Friml et al., 2003). The fact that the same patterning defects are observed in *Arabidopsis* mutants in members of the *PIN* gene family, such as *pin1* and the *pin4 pin7* double mutant (Liu et al., 1993; Friml et al., 2002, 2003), supports the requirement of PIN-dependent PAT for normal embryo patterning.

Expression of the auxin-dependent reporter DR5rev green fluorescent protein (*DR5rev-GFP*) indicates dynamic changes in auxin distribution during specific patterning events in the embryo

[1] To whom correspondence should be addressed. E-mail offringa@rulbim.leidenuniv.nl; fax 31-71-5274999.
The author responsible for distribution of materials integral to the findings presented in this article in accordance with the policy described in the Instructions for Authors (www.plantcell.org) is: Remko Offringa (offringa@rulbim.leidenuniv.nl).
[W] Online version contains Web-only data.
Article, publication date, and citation information can be found at www.plantcell.org/cgi/doi/10.1105/tpc.105.034637.

(Friml et al., 2003). Initially, *DR5rev-GFP* activity localizes to the proembryo, and later it shifts basally to the hypophysis. This dynamic distribution of auxin activity in the embryo, for simplicity here referred to as auxin gradients, depends on PIN-mediated auxin transport. Although it is now relatively well understood how auxin gradients are established and how they might be translated into gene expression patterns by the auxin response protein MONOPTEROS/AUXIN RESPONSE FACTOR5 (Hardtke and Berleth, 1998) and its inhibitor BODENLOS/INDOLEACETIC ACID12 (Hamann et al., 2002), it is yet unknown how robust auxin gradients are and by which mechanisms they are maintained. This could involve local auxin biosynthesis and degradation, auxin transport, or a combination of both.

Here, we show that neither enhancing the rate of auxin biosynthesis nor manipulation of auxin conjugation rates changed auxin gradients or embryo patterning, revealing a robust buffering mechanism. This buffering capacity depends critically on PIN-dependent PAT, suggesting that in addition to establishing auxin gradients, auxin transport also maintains these gradients during embryogenesis.

RESULTS

Manipulation of Auxin Homeostasis

Bacterial enzymes were conditionally expressed to modify cellular auxin concentrations in developing zygotic embryos. The *Agrobacterium tumefaciens indoleacetic acid-tryptophan monooxygenase* (*iaaM*) gene encodes an enzyme that catalyzes the conversion of Trp into indole-3-acetamide, which is hydrolyzed to indole-3-acetic acid (IAA) in plant cells (Klee et al., 1987; Romano et al., 1995). The *Pseudomonas syringae indoleacetic acid-lysine synthetase* (*iaaL*) gene encodes an enzyme that converts IAA and Lys into the biologically inactive IAA-Lys conjugate, and its expression results in a decrease of the levels of free IAA in plant cells (Romano et al., 1991). *iaaM* or *iaaL* expression generally causes cellular auxin concentration changes of 2- to 10-fold (Klee et al., 1987; Romano et al., 1991, 1995), well within the physiological range.

The *iaaM* and *iaaL* genes were introduced into a GAL4 transcription factor/Upstream (GAL4/*UAS*) two-component gene expression system optimized for use in *Arabidopsis* (Weijers et al., 2003). A UAS-driven GFP-β-glucuronidase (*UAS-GFP*:*GUS*) reporter gene was linked to the *UAS-iaaM* or *UAS-iaaL* genes to monitor expression of *iaaM* or *iaaL*. We have previously shown that this transactivation system is reliable and reproducible for domain-specific expression in *Arabidopsis* seeds (Weijers et al., 2003). As expected, *UAS-iaaM*;*UAS-GFP*:*GUS* (EF *iaaM*) and *UAS-iaaL*;*UAS-GFP*:*GUS* (EF *iaaL*) lines did not express the *iaaM* or *iaaL* mRNAs (see Supplemental Figure 1 online) and were wild-type in appearance.

To first assess whether this approach allows changing cellular auxin concentrations, we crossed EF *iaaM* and EF *iaaL* lines with an ACT LIPID TRANSFER PROTEIN1 (*proLTP1*) line that expresses GAL4 in the epidermis (Weijers et al., 2003) and analyzed postembryonic development.

The effects of *iaaM* expression on postembryonic development have been described in detail for *Arabidopsis* (Romano et al., 1995), tobacco (*Nicotiana tabacum*; Sitbon et al., 1992), and petunia (*Petunia hybrida*; Klee et al., 1987). In accordance with these studies, hypocotyl elongation was strongly enhanced in *proLTP1≫iaaM* seedlings (the notation *proX≫Y* describes transactivation of gene Y by promoter X; average hypocotyl length 1.66 ± 0.24 mm [$n = 26$] in the wild type, 4.61 ± 0.86 mm [$n = 30$] in *proLTP1≫iaaM*; Figure 1A). Such seedlings showed several other hallmarks of auxin overproduction, such as epinastic cotyledons and long petioles (Figure 1A). Upon rosette leaf formation, *proLTP1≫iaaM* phenotypes became more extreme, with leaves becoming epinastic and narrow (Figure 1B). Inflorescences were less branched, produced few flowers, and often terminated into a pin-like structure bearing only a few flower buds (Figure 1B; see Supplemental Figure 2 online). Measurement of free auxin levels in *proLTP1≫iaaM* plants showed that concentrations were elevated severalfold (Figure 1B).

Genetically identical *proLTP1≫iaaM* F1 plants showed variable strength of auxin-related phenotypes. We have shown previously that when using the GAL4/*UAS* system, gene expression levels may vary strongly between genetically identical sibling embryos (Weijers et al., 2003). The mechanism behind this phenomenon is not clear, but nonetheless we exploited this variability to correlate variations in phenotypes to auxin concentrations and to justify the use of the *GFP*:*GUS* reporter gene as marker for *iaaM* activity. The phenotypic strength clearly correlated with the free auxin levels, the strongest phenotypic class of plants showing as much as a sixfold increase in auxin concentration (Figure 1B). This increase is considerable since the *LTP1* promoter is only active in epidermal cells of growing aerial organs. GUS activity also increased with auxin levels and phenotypic strength, thereby reinforcing that *iaaM* activity is reflected by activity of the coactivated *GFP*:*GUS* reporter gene.

As expected from previous reports (Gray et al., 1998; Zhao et al., 2001), *proLTP1≫iaaL* expression had the opposite effect on seedling and plant phenotype as *proLTP1≫iaaM* expression. Cotyledon expansion was increased, and hypocotyl length and root growth were decreased (Figure 1C). Furthermore, *proLTP1≫iaaL* seedlings showed altered response to gravity (Figure 1D), and flowering plants displayed a decrease of apical dominance (see Supplemental Figure 2 online). Taken together, postembryonic phenotypes and auxin concentration measurements show that GAL4/*UAS*-mediated expression of the *iaaM* and *iaaL* genes allows manipulating auxin homeostasis and that the induced changes are sufficient for altering postembryonic plant development.

Embryo Patterning Is Not Affected by Enhanced Auxin Biosynthesis or Conjugation

To assess the effects of local changes in auxin homeostasis on embryo pattern formation, preselected EF *iaaM* and EF *iaaL* lines (Table 1) were crossed to a range of lines, each expressing GAL4 in a subset of embryonic cells.

Strikingly, no pattern defects were observed when *iaaM* or *iaaL* were expressed from the strong embryonic RIBOSOMAL PROTEIN S5 (*RPS5A*) promoter (Weijers et al., 2001, 2003) at stages ranging from two-cell to torpedo stage (Figures 2A, 2B, 2G, and 2H, Table 2).

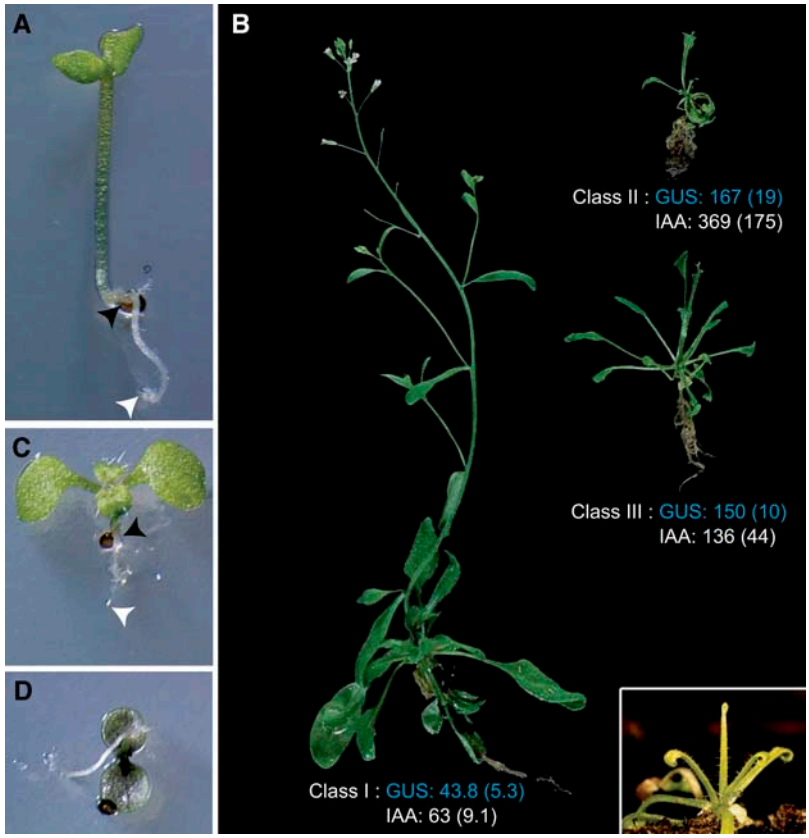

Figure 1. Manipulation of Auxin Concentrations by *iaaM* or *iaaL* Expression.

(A) A 5-d-old pro*LTP1*≫*iaaM* F1 seedling showing a long hypocotyl and small epinastic cotyledons.
(B) Three 4-week-old pro*LTP1*≫*iaaM* F1 plants representing the different classes (I, II, and III) of iaaM-induced phenotypes. Free IAA concentration (pg/mg fresh weight, white numbers) and GUS activity (pmol 4-methyl umbelliferone/mg protein/min, blue numbers) are indicated for each phenotypic class. The number in parentheses indicates the standard error of the mean. Inset shows a pro*LTP1*≫*iaaM* F1 plant with a pin-like inflorescence structure.
(C) A 5-d-old pro*LTP1*≫*iaaL* F1 seedling showing large cotyledons and a short hypocotyl and root. The hypocotyl-root junction and the root tip in **(A)** and **(C)** are marked with black and white arrowheads, respectively.
(D) A 5-d-old pro*LTP1*≫*iaaL* F1 seedling growing upside down indicates a defect in gravitropic growth.

In addition to *proRPS5A*, a number of promoters were used to drive *iaaM* or *iaaL* expression in restricted domains of the embryo or seed. The *LTP1* promoter was used for expression in the apical protoderm (Thoma et al., 1994; Vroemen et al., 1996; Figures 2C and 2I). Expression in the suspensor was achieved by crossing with a line expressing GAL4 from a suspensor-specific promoter fragment (Figures 2D and 2J; D. Weijers and R. Offringa, unpublished data) of the *SHOOT MERISTEMLESS* (*STM*) gene (Long et al., 1996) or from GAL4 enhancer trap lines J3281 and M0167 (Figures 2F and 2L; www.plantsci.cam.ac.uk). *iaaM* and *iaaL* were expressed in the central embryo domain using GAL4 enhancer trap line Q0990 (www.plantsci.cam.ac.uk; Figures 2E and 2K) and in an auxin-dependent fashion using the *DR5*(*7x*) promoter (Ulmasov et al., 1997). Finally, the genes were expressed in endosperm using GAL4 enhancer trap line KS22I (Boisnard-Lorig et al., 2001).

In each of the crosses of the selected GAL4 lines and *iaaM* or *iaaL* lines, the *UAS*-dependent *GUS* or *GFP* reporter genes were correctly expressed (Figure 2). None of these genotypes, however, caused changes in embryo pattern formation (Figure 1, Table 2; for the genotypes that are not listed in Table 2, at least 100 embryos were analyzed). These results indicate that in contrast with the strong effects on postembryonic development, manipulation of auxin biosynthesis or conjugation activity do not alter embryo patterning, suggesting the existence of mechanisms that buffer the changes in auxin homeostasis in the embryo.

Enhanced Auxin Biosynthesis or Conjugation Rates Leave Embryonic Auxin Gradients Unaffected

The absence of *iaaM*- or *iaaL*-induced embryo phenotypes could mean that the genes, despite their postembryonic activity, are not functional or lack substrates during embryogenesis. Alternatively, the enzymes are active and auxin levels are changed in transgenic embryos, but the patterning mechanism is buffered against changes in auxin levels. As direct auxin concentration

Table 1. Frequencies of Embryo Pattern Defects in the Parental Lines and Control Crosses

Plant Lines	Generation[a]	Self-Pollination [% (d/n)] [b]	Cross-Pollination [% (d/n)][b,c]
Columbia wild-type, experiment 1	–	2.9% (3/102)	–
Columbia wild-type, experiment 2	–	0.8% (1/121)	–
ACT *proRPS5A*#5	T4, hom	0.6% (1/166)	1.8% (2/110)
ACT *proDR5*(*7x*)#3	T3, hom	2.3% (5/219)	–
ACT *proLTP1*#8	T4, hom	0.9% (1/109)	3.2% (1/31)
EF *iaaM*#3	T3, hom	<0.9% (0/109)	0.6% (1/181)
EF *iaaM*#5	T2	<0.5% (0/201)	<1.2% (0/82)
EF *iaaM*#9	T2	<1.2% (0/80)	<1.3% (0/78)
EF *iaaM*#10	T2	2.9% (7/242)	1.0% (1/99)
EF *iaaL*#3	T2	<0.4% (0/250)	<1.4% (0/67)
EF *iaaL*#8	T2	<0.5% (0/179)	0.8% (1/124)
EF *iaaL*#11	T3, hom	<0.7% (0/138)	<1.3% (0/74)
EF *iaaL*#18	T2	<0.7% (0/138)	<1.1% (0/93)
pin4-3; ACT *proRPS5A*#5	F3	0.7% (2/275)	–
pin4-3; EF *iaaM*#3	F3	<0.9% (0/111)	–
pin4-3; EF *iaaL*#11	F3	ND[d]	–

[a] For several lines, homozygous (hom) plants were selected in the T3 or T4 generation. For most EF lines, T2 generation plants were used, and in this case, deviations in embryo pattern were scored in the same T2 plant that was used for crosses.

[b] Defects were defined as obvious changes in the pattern of the hypophyseal cell group (the majority of the abnormalities), changes in the number of cotyledons, or the occurrence of fused cotyledons at globular and heart stages. Small changes in embryo size were not taken into account. Changes in the apical pattern were only rarely found (<5% of the defects). The percentage of defective embryos (%), as well as the number of defective embryos (d) and the total number of analyzed embryos (n) is given.

[c] Plants were used as a male (EF lines) or female (ACT lines) parent in a cross with Columbia wild-type plants.

[d] ND, not determined.

measurements on young embryos are not yet feasible, and immunolocalization of auxin is not quantitative, we used a combination of other approaches to discriminate between these possibilities. First, we analyzed the activity of the auxin-dependent *DR5rev-GFP* reporter gene (Friml et al., 2003) in embryos expressing *iaaM* or *iaaL*. The *DR5rev-GFP* reporter was crossed into ACT *proRPS5A*, ACT *proLTP1*, and EF *iaaM* and EF *iaaL* lines, and plants carrying both transgenes were selected and used in crosses.

Consistent with the reported activity of the iaaM enzyme, *proRPS5A*≫*iaaM* embryos and seedling roots showed enhanced *DR5rev-GFP* signals (Figures 3A, 3B, 3G, and 3H). However, the enhanced signals were restricted to cells that normally express the marker in control embryos. To test whether other cells in

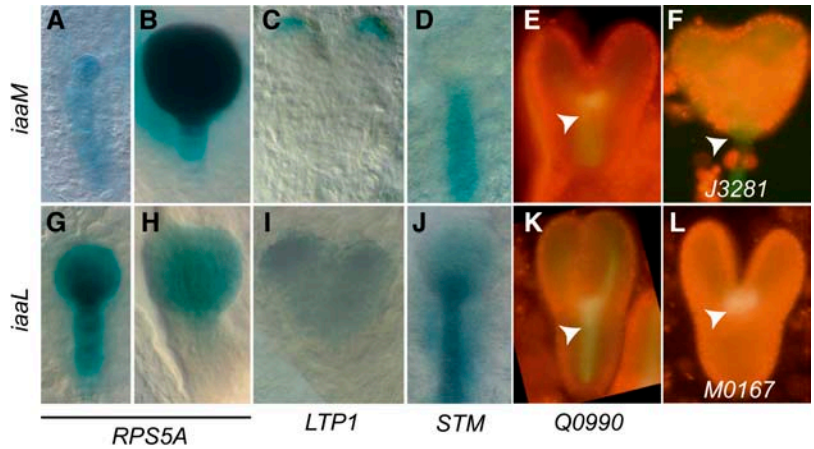

Figure 2. Expression of *iaaM* or *iaaL* in the *Arabidopsis* Embryo.

F1 embryos resulting from crosses between EF *iaaM* (**[A]** to **[F]**) or EF *iaaL* (**[G]** to **[L]**) plants and ACT pro*RPS5A* (**[A]**, **[B]**, **[G]**, and **[H]**), ACT pro*LTP1* (**[C]** and **[I]**), ACT po*STM* (**[D]** and **[J]**), Q0990 (**[E]** and **[K]**), J3281 **(F)**, or M0167 **(L)** lines. Embryos in **(A)** to **(D)** and **(G)** to **(J)** were stained for up to 18 h for GUS activity. Despite strong GAL4:VP16-dependent gene activation, as reported by the GUS activity, embryos show a wild-type phenotype. Embryos in **(E)**, **(F)**, **(K)**, and **(L)** were observed under an epifluorescence microscope. The green signal (arrowheads, central tissues in **[E]** and **[K]**; suspensor in **[F]**, and shoot apical meristem region in **[L]**) marks activity of the GAL4:VP16-dependent *mGFP5-ER* reporter gene.

Table 2. *iaaM* and *iaaL* Expression Induces Embryo Pattern Defects in *pin4* but Not in Wild-Type Embryos

	Transactivation in F1 Progeny[a]		Embryo Pattern Defects [% (d/n)][b]	
Plant Lines	GUS	Exp.	Apical	Basal
proRPS5A#5≫*iaaM*#3	6/6	100%	1.0% (1/100)	1.0% (1/100)
proRPS5A#5≫*iaaM*#5	21/45	50%	<1.3% (0/77)	1.3% (1/77)
proRPS5A#5≫*iaaM*#9	23/48	50%	<0.7% (0/136)	0.7% (0/136)
proRPS5A#5≫*iaaM*#10	30/30	100%	2.0% (4/197)[c]	2.0% (4/197)[c]
proRPS5A#5≫*iaaL*#3[d]	4/28	25%	0.8% (1/123)[e]	3.2% (4/123)[e]
proRPS5A#5≫*iaaL*#3[d]	ND[f]	50%	<2.8% (0/36)	<2.8% (0/36)
proRPS5A#5≫*iaaL*#8	19/39	50%	3.1% (5/163)	0.6% (1/163)
proRPS5A#5≫*iaaL*#11	34/34	100%	<0,8% (0/130)	<0,8% (0/130)
proRPS5A#5≫*iaaL*#18	12/28	50%	<1.3% (0/74)	2.7% (2/74)
proDR5(*7x*)#3≫*GGi*#15	24/95	100%	ND	ND
proDR5(*7x*)#3≫*iaaM*#3	n.t.	100%	<1.8% (0/55)	1.8% (1/55)
proDR5(*7x*)#3≫*iaaL*#3	n.t.	50%	<1.8% (0/54)	<1.8% (0/54)
proDR5(*7x*)#3≫*iaaL*#11	7/176	100%	<1.1% (0/89)	<1.1% (0/89)
proLTP1#8≫*iaaM*#3	n.t.	100%	<3.2% (0/31)	<3.2% (0/31)
proLTP1#8≫*iaaM*#5	n.t.	50%	<2.8% (0/35)	<2.8% (0/35)
proLTP1#8≫*iaaL*#3	n.t.	50%	<2.3% (0/44)	<2.3% (0/44)
proLTP1#8≫*iaaL*#11	n.t.	100%	<3.4% (0/29)	<3.4% (0/29)
pin4-3; *proRPS5A*#5≫*iaaM*#3	n.t.	100%	8.9% (23/257)	0.8% (2/257)
pin4-3; *proRPS5A*#5≫*iaaL*#11	n.t.	100%	0.7% (1/147)	32% (47/147)

[a] When the genotypes of the parental plants were not known, the frequency of transactivation was tested by analyzing GUS activity in all embryos from one or two siliques. The number of GUS-positive embryos is indicated per total number of embryos analyzed (n.t., not tested because the genotype of the parental plants is known). The second column indicates the percentage of *iaaM*- or *iaaL*-expressing embryos that can be expected based on GUS staining of embryos and/or known genotype of the parental plants.

[b] The embryo pattern defects are defined in the legend of Table 1.

[c] This frequency represents the added results of three independent crosses between the same parent plants. The respective frequencies in each cross were 17% (6/36), 1.9% (2/106). and <1.8% (0/55). The phenotypes observed in the first cross were hypophyseal cell group defects ($n = 4$) and irregularly short cotyledons ($n = 2$).

[d] Results from two independent crosses are shown: in the first cross, a hemizygous ACT *proRPS5A#5* plant was used. In the second cross, a homozygous ACT *proRPS5A#5* plant was used.

[e] The phenotypes in this cross were hypophyseal cell group defects ($n = 4$) and irregular cotyledon pattern ($n = 1$).

[f] ND, not determined.

proRPS5A≫*iaaM* embryos also contain elevated auxin concentrations that might not be sufficient to activate the *DR5rev-GFP* reporter, embryos were treated with 10 μM of the synthetic auxin 2,4-D. Whereas 2,4-D treatment enhanced the *DR5rev-GFP* activity peak only in the basal region in wild-type embryos (Figure 3C), in *proRPS5A*≫*iaaM* embryos, the signal was increased in both the basal region and the provascular tissues (Figure 3I). The lower threshold auxin concentration for induction of the *DR5rev* promoter in *proRPS5A*≫*iaaM* embryos indicates that iaaM is also active in these cells and its substrate is not limiting for enhanced auxin biosynthesis. Exogenous application of high concentrations (1 mM) of Trp to developing seeds enhanced the *DR5rev-GFP* signal in *iaaM*-expressing embryos (Figure 3J) but not in wild-type embryos (Figure 3D). This corroborates our previous conclusion that the *iaaM* embryos express an active iaaM enzyme that is able to convert the Trp substrate into the auxin precursor indolacetamide. Although expression of the coregulated *GUS* gene in *proDR5*(*7x*)≫*iaaL* embryos (Table 2) was strongly reduced compared with *proDR5*(*7x*)≫*GUS* control embryos (Table 2), this reduced auxin activity could not be confirmed using the *DR5rev-GFP* reporter, even when embryos were cultured in medium containing Lys, auxin, or auxin transport inhibitors (see Supplemental Figure 3 online). It can therefore not be directly shown that iaaL is effective in embryos.

PAT Activity Buffers Auxin Gradients for Embryo Patterning

It has previously been shown that most cells in the embryo can respond to auxin by switching on the *DR5rev-GFP* marker (Friml et al., 2003). Surprisingly, the expression of *iaaM* from the strong ubiquitous *RPS5A* promoter caused enhanced auxin levels/activity only in those cells that normally express the marker; consequently, *iaaM*-expressing embryos are normal in phenotype. This suggests that embryos can regulate the activity or distribution of excess auxin to maintain the existing auxin gradients.

Maintenance of such gradients in the seedling root requires PAT activity (Friml et al., 2002). To test whether an auxin transport-dependent mechanism also operates to maintain embryonic auxin gradients, immature seeds containing either wild-type or *proRPS5A*≫*iaaM* embryos were cultured on growth media containing different concentrations of the PAT inhibitor NPA. If PAT is responsible for maintaining auxin levels in the proembryo at concentrations that allow normal pattern formation, treatment of *proRPS5A*≫*iaaM* F1 seeds with NPA is expected to lead to

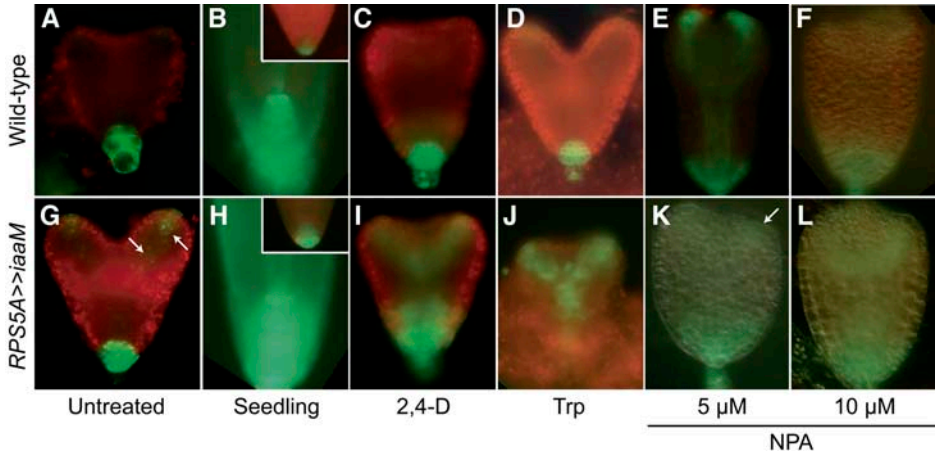

Figure 3. *DR5rev-GFP* Activity in in Vitro–Cultured *iaaM*-Expressing Embryos.

DR5rev-GFP reporter gene activity (green) in wild-type (**[A]** to **[F]**) and pro*RPS5A*≫*iaaM* F1 (**[G]** to **[L]**) embryos (**[A]**, **[C]** to **[G]**, and **[I]** to **[L]**) and seedling root tips (**[B]** and **[H]**).

(A) and **(G)** Embryos cultured on unsupplemented medium for 2 d. The pro*RPS5A*≫*iaaM* embryo shows enhanced fluorescence in the root tip and in the cotyledon tips and provascular cells (arrows).

(B) and **(H)** Root tips from 4-d-old seedlings germinated on solid growth medium. Insets show root tip regions of corresponding mature embryos. Note that pro*RPS5A*≫*iaaM* embryonic and seedling roots show enhanced GFP fluorescence.

(C) and **(I)** Embryos prepared from seeds that were cultured during 2 d in the presence of 10 μM 2,4-D. Note the enhanced and expanded fluorescence in both embryos.

(D) and **(J)** Embryos prepared from immature seeds that were cultured during 3 d in the presence of 1 mM Trp. Note that Trp does not change *DR5rev-GFP* activity in the wild type but strongly enhances fluorescence in pro*RPS5A*≫*iaaM* embryos.

(E), **(F)**, **(K)**, and **(L)** Embryos prepared from seeds that were cultured during 3 d in the presence of 5 μM (**[E]** and **[K]**) or 10 μM (**[F]** and **[L]**) NPA. Note that the wild-type embryo in **(E)** has fully separated cotyledons, while the pro*RPS5A*≫*iaaM* embryo in **(K)** has fused cotyledons (arrow). With 10 μM NPA, both embryos have completely fused cotyledons (**[F]** and **[L]**).

increased accumulation of auxin and thus to embryo phenotypes at lower NPA concentrations compared with the wild type. Culturing with 5 μM NPA enhanced the *DR5rev-GFP* signal in wild-type embryos (Figure 3E) but did not alter the embryo pattern, whereas only higher (up to 20 μM) concentrations caused fusion of cotyledons (Friml et al., 2003; Figure 3F). By contrast, treatment of *proRPS5A*≫*iaaM* F1 seeds with 5 μM NPA led to nearly complete fusion of cotyledons (Figures 3K and 3L), indicating that pattern formation in *proRPS5A*≫*iaaM* embryos is sensitized to inhibition of PAT. This result indicates that PAT activity buffers the normal distribution of auxin when auxin biosynthesis rates are changed.

PINs Maintain an Auxin Distribution Required for Apical and Basal Embryo Patterning

Four PIN proteins are active in the *Arabidopsis* embryo (Friml et al., 2003; Blilou et al., 2005). PIN7 is required for establishment of the preglobular auxin gradient, while PIN1 is involved in its reversal during the globular stage. PIN4 is expressed immediately after reversal of the gradient, and PIN3 is expressed even later (Friml et al., 2003).

Hence, the PINs most likely to be involved in maintenance of auxin gradients during the stages analyzed above are PIN1 and PIN4. To test whether these proteins are indeed involved in maintenance of auxin gradients, the sensitivity of *pin* mutant embryos to exogenously applied 1-naphthylacetic acid (1-NAA) was compared with that of wild-type embryos. Immature *pin1-3* or *pin4-3* mutant seeds, as well as seeds from wild-type plants, were cultured in the presence of 1-NAA or on control medium. Approximately half of the embryos homozygous for the *pin1-3* mutation show weak fusion of cotyledons (Aida et al., 2002). A similar frequency of weak cotyledon fusion was observed when *pin1-3* embryos were cultured on control media (Figure 4A). When cultured on 1-NAA, however, these apical defects were strongly enhanced and included complete fusion of cotyledons (Figure 4B). Similarly, whereas *pin4-3* embryos have no apical embryonic defects (Figures 4C and 4D), culturing on 1-NAA induced apical asymmetry and cotyledon fusion (Figure 4E). These results suggest that both PIN1 and PIN4 are involved in maintaining the embryonic auxin gradient.

To study the activity of PINs in gradient maintenance in conditions where auxin levels are genetically enhanced or decreased, we crossed ACT *proRPS5A* and EF *iaaM* and *iaaL* transgenes into the *pin4-3* mutant. This mutant was chosen because in contrast with *pin1-3*, it has only very weak embryo defects of its own (Friml et al, 2002), thus facilitating the interpretation of possible *iaaM*- or *iaaL*-induced pattern defects. Strikingly, while all controls showed <1% abnormal embryos (Table 1, Figure 4F), 9% of the *pin4-3*;*proRPS5A*≫*iaaM* embryos showed fusion of cotyledons (Figures 4G and 4H; Table 2). This result indicates that PIN4-mediated auxin transport is required to control auxin concentrations in the proembryo to allow apical patterning. Development of the basal embryo pole was not

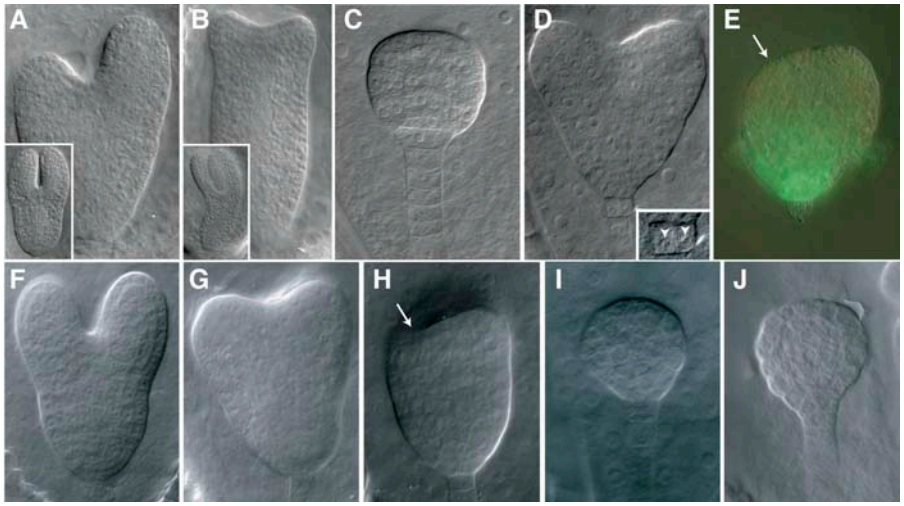

Figure 4. *pin1-3* and *pin4-3* Mutants Are Hypersensitive to Alterations in Auxin Homeostasis.

(A) and **(B)** *pin1-3* embryo grown on control medium **(A)** or in the presence of 5 μM 1-NAA **(B)**. Insets show wild-type embryos grown under identical conditions. Note the reduction and complete fusion of cotyledons in the *pin1-3* embryo on 1-NAA–containing medium.
(C) and **(D)** Globular stage **(C)** and heart stage **(D)** *pin4-3* embryos. Inset in **(D)** shows a magnification of the vertically divided apical-most suspensor cell (arrowheads indicate both nuclei).
(E) *DR5rev-GFP* expression in a *pin4-3* heart stage embryo cultured in the presence of 5 μM 1-NAA. Note the enhanced GFP fluorescence in the apical region of the embryo (as compared with the wild-type embryo in Figure 3A) and the fusion of cotyledons (arrow).
(F) Wild-type late heart stage embryo.
(G) and **(H)** *RPS5A≫iaaM*; *pin4-3* heart stage embryos showing fusion of cotyledons (arrow).
(I) and **(J)** *RPS5A≫iaaL*; *pin4-3* embryos showing a disorganized basal pole.

affected by *proRPS5A≫iaaM* expression in *pin4-3* embryos (Figures 4G and 4H; Table 2). Likewise, the basal embryo pole developed normally when *pin4-3* embryos were cultured in the presence of 1-NAA (Figure 4E). By contrast, 25% of the *pin4-3*; *proRPS5A≫iaaL* embryos showed deformations of the root pole at the late globular stage (Figures 4I and 4J). This result provides evidence that the *iaaL* gene is active in the embryo and more importantly that free auxin is required for regulation of division patterns in the basal region of the globular *Arabidopsis* embryo. In addition, these results show that PIN4 activity in the embryo maintains a differential distribution of auxin between the proembryo and hypophysis, which on one hand allows apical patterning and on the other hand regulates root pole patterning.

DISCUSSION

Designed to copy the body organization of the parent, embryogenesis is a crucial step in the life cycle of a plant. Although the timing and regularity of patterning and the final size of embryos can differ considerably between plant species (Johri et al., 1992), the general uniformity of the final shape suggests a robust and tightly controlled underlying regulatory mechanism. Pharmacological studies on embryos of several plant species and genetic studies in *Arabidopsis* have suggested an important role for auxin in the regulation of plant embryogenesis. Auxin activity, as measured by the expression of an auxin-dependent reporter gene, is highly dynamic during *Arabidopsis* embryogenesis, and the establishment of auxin gradients requires an intact polar transport system (Friml et al., 2003). Here, we have studied how these gradients are maintained. Our findings show that auxin biosynthesis and inactivation rates can be modified without an effect on auxin gradients or on pattern formation. However, altering auxin biosynthesis or conjugation rates under conditions where auxin transport is compromised inflicts changes in auxin gradients and embryo patterning. Our results show that auxin transport is crucial for maintenance of embryonic auxin gradients during pattern formation.

Embryonic Auxin Gradients and Pattern Formation Are Robustly Buffered

Postembryonic manipulation of auxin homeostasis using bacterial enzymes effectively alters auxin-mediated plant development, including elongation of hypopcotyl and petioles, outgrowth of lateral buds, and initiation of flowers (Romano et al., 1991, 1995; this report). It has recently been established that pattern formation in plant embryos also involves auxin activity. Nonetheless, strong expression of the same bacterial enzymes that interfere with postembryonic development does not interfere with embryo patterning. Because both the iaaM auxin biosynthesis enzyme and the iaaL auxin conjugation enzyme use an amino acid as a substrate, a trivial explanation would be that the substrate for these enzymes is lacking in embryos, whereas it is available postembryonically. Because of the fast growth rate of embryos and the associated requirement for de novo protein synthesis (Weijers et al., 2001), amino acids should be available in abundance. Yet it is conceivable that despite abundance,

there is no excess and that most amino acids are efficiently shuttled into the protein biosynthesis pathway. Visualizing auxin distribution indirectly, using an auxin responsive reporter gene, showed that iaaM expression does increase cellular auxin concentrations. Additional Trp feeding experiments showed that Trp is used as a substrate and that endogenous Trp concentrations are not saturating for maximal iaaM activity. Nonetheless, the absence of iaaM-induced embryo defects is not due to unavailability of the Trp substrate but rather involves a mechanism that buffers the patterning process from alterations in cellular auxin concentration. For the iaaL enzyme, which uses Lys to inactivate IAA, we obtained indirect evidence for its activity in embryos. iaaL expression only affects auxin levels (as measured by altered auxin-dependent pattern formation) if auxin transport activity is compromised, and under those conditions, Lys concentrations in the embryo are clearly not limiting to its activity.

A buffering mechanism for auxin activity could involve flexible adaptation of de novo auxin biosynthesis, auxin inactivation, or auxin transport. The first two mechanisms are not well understood at the molecular level, and identification and functional analysis of critical components for auxin catabolism and biosynthesis in the embryo will be required to assess the exact contribution of these pathways. We found that PAT activity is crucial for maintaining embryonic auxin gradients when cellular auxin concentrations are changed.

Particularly, we observed that at least two of the embryonically active PIN proteins, PIN1 and PIN4, act in maintaining such gradients. This suggests that differential auxin distribution requires the continuous activity of PIN proteins in order to compensate for fluctuations in cellular auxin concentrations. Several interpretations could account for the flexible regulation of auxin transport activity, one being that differences in auxin concentration between adjacent cells are sensed and feed back on auxin efflux activity. Alternatively, cell-autonomous auxin-dependent regulation of PIN expression or activity could account for the observed flexibility.

It is likely that, in addition to auxin transport, other cellular homeostasis mechanisms contribute to maintenance of auxin gradients. When more auxin is transported to the maximum of the gradient, more auxin has to be inactivated there. Thus, robustness in auxin gradient maintenance will also require flexibility in auxin biosynthesis and degradation machinery, whose local activity is adjusted to the amount of auxin flowing through the gradient. Although this has not experimentally been tested, embryos may have considerable auxin biosynthesis and conjugation capacity.

PIN4 Fulfills a Similar Function in the Embryo and Seedling Root

Our results reveal a new function for PIN4 in the maintenance of embryonic auxin gradients. This function is not apparent during normal development of the *pin4* mutant but is uncovered when mutant embryos are challenged with elevated or decreased auxin concentrations. It is difficult to judge what variations in auxin concentrations normally occur in plant development. Nonetheless, PIN4 function, in addition to that of PIN1, ensures that whatever variations exist, the shape of the embryonic auxin gradient is not altered.

There is an interesting parallel between the embryonic and the postembryonic PIN4 function. In postembryonic root tips, PIN4 is expressed in the quiescent center and the surrounding stem cells where it focuses auxin transport to form a *DR5rev* activity peak (Sabatini et al., 1999; Friml et al., 2002). In the *pin4* loss-of-function mutant, *DR5rev* activity is still focused below the quiescent center, but it is generally enhanced and detectable in more distal cells, correlating with the elevated auxin concentrations in *pin4* root tips (Friml et al., 2002). Likewise, in *pin4* mutant embryos, *DR5rev* activity, which is normally restricted to the hypophysis derivatives in the wild type, is observed in the apical half of the embryo. Thus, in both situations, a localized activity of PIN4 at or adjacent to the maximum of the auxin gradient is required to prevent accumulation of auxin in distal cells. Although it has been suggested that auxin catabolism is induced in the auxin maximum in root tips (Jiang et al., 2003), at present it is unclear how such feedback control works, and better understanding will require the dissection of PIN protein activity and the identification of the regulators of these proteins.

Concluding Remarks

This work has identified that auxin-dependent pattern formation of plant embryos is highly flexible, in that it can accommodate changes in auxin levels without affecting the dynamic auxin gradients or pattern formation in the embryo. Our results show that the PIN auxin efflux facilitators not only play a central role in the establishment of these auxin gradients but that they are essential components in their robust maintenance as well. In view of our findings, there is a striking parallel between the responsiveness of embryonic and postembryonic auxin-dependent processes toward altered auxin concentrations and the degree to which the same processes can be modulated by environmental conditions. A future challenge will be to identify how other auxin homeostasis mechanisms are linked to the PIN auxin efflux network to create this robust buffering system.

METHODS

Growth of Plants and Genetic Crosses

Arabidopsis thaliana ecotype Columbia was used as a wild type in all experiments. Seed sterilization, plant growth, and transformation (Weijers et al., 2001) and in vitro culturing of immature seeds (Friml et al., 2003) were performed as described. The *pin4-3* mutant and *DR5rev-GFP* line were described previously (Friml et al., 2002, 2003). GAL4 enhancer trap lines Q0990, J3281, and M0167 were obtained from the Nottingham Arabidopsis Stock Centre. The KS22I enhancer trap line has been described previously (Boisnard-Lorig et al., 2001).

For crossing experiments, T2 to T4 generation plants were used. Homozygotes for the T-DNA insertion locus were selected in the T3 and T4 generations. When T2 generation EF lines were used in crosses, a test cross between a single transgenic plant and a homozygous ACT *RPS5A*#5 line was performed to determine the frequency of GUS-positive embryos. The same plant was then used for subsequent crossing experiments. ACT lines and wild-type plants were used as female parents in all crosses, unless indicated otherwise.

Ovule culture experiments were performed as described (Sauer and Friml, 2004) using F1 seeds directly after crossing of ACT *proRPS5A*

DR5rev-GFP and EF *iaaM DR5rev-GFP* plants or on a line homozygous for *pin4-3* and *DR5rev-GFP*. Controls were parental lines used for crosses. Media were supplemented with 1-NAA (Duchefa; 5 or 10 μM), 2,4-D (Duchefa; 10 μM), NPA (Duchefa; 5 or 10 μM), or Trp (Roth; 1 mM).

T-DNA Constructs, Transgenic Plants, and Selection of Lines

All ACT lines except ACT *proSTM* and the EF *GGi* lines have been described (Weijers et al., 2003). For ACT *proSTM*, a 1.5-kb region upstream of the ATG start codon of the *Arabidopsis STM* gene (Long et al., 1996) was amplified with primers STM-5-HD1 (5′-GCAAGCTTCAGGGATAAACAGGTACAGG-3′) and STM-3-BH1 (5′-CCGGATCCCTTCTCTTTCTCTCACTAG-3′) with added *Hin*DIII and *Bam*HI sites (underlined), subcloned in pBluescript SK+, and cloned as a *Hin*DIII-*Bam*HI fragment upstream of *mGAL4*:*VP16* in pSDM1600.

The *iaaM* coding region (position 5762 to 8076 according to Barker et al., 1983) was amplified by PCR from Ti plasmid pTi15955 using Expand Taq polymerase (Roche Molecular Biochemicals) and the primers iaaM-F (5′-CGGTTGATGTGGTTATTTATCTACAC-3′) and iaaMSacR (5′-ACGAGCTCCTAATTTCTAGTGCGGTAG-3′). The 2.3-kb PCR fragment was sequenced, digested with *Sac*I, and cloned into the *Eco*RV-*Sac*I sites of pSDM7022 (Weijers et al., 2003) to yield pIC *proUAS-iaaM-tNOS* (pSDM7009). A 2.7-kb *Hin*dIII fragment containing *proUAS-iaaM-tNOS* was cloned into pSDM7006 (Weijers et al., 2003) to yield pEF *iaaM* (pSDM7010). The *iaaL* coding region was isolated as part of a 1.8-kb *Bgl*II-*Bam*HI *iaaL-tNOS* fragment from pMON690 (Romano et al., 1991) and fused to *proUAS* in pSDM7000 to yield pSDM7011 (Weijers et al., 2003). Next, the *UAS-iaaL-tNOS* cassette was isolated as a *Hin*dIII fragment and ligated into pSDM7006 to yield EF *iaaL* (pSDM7012). (Unfortunately, due to the license policy of Monsanto, no *iaaL* derivative constructs or plant lines can be distributed.) Constructs were electroporated into *Agrobacterium tumefaciens* strain LBA1115 as described previously (Weijers et al., 2001). Transgenic lines were analyzed in the T2 generation. To estimate the number of T-DNA copies in EF lines, DNA gel blot analysis was performed as described (Weijers et al., 2003) using gene-specific probes and a *GFP* probe. RT-PCR was performed on RNA isolated from young siliques using primer sets specific for *iaaM* or *iaaL*. The lines used for experiments (unless indicated otherwise) are as follows: ACT *proRPS5A*#5, ACT *proLTP1*#8, ACT *proSTM*#6, ACT *proDR5*(*7X*)#3, EF *GFP:GUS*#15, EF *iaaM*#5, and EF *iaaL*#18.

Auxin Quantification

proLTP1#8≫*iaaM*#20 F1 seeds were germinated on soft agar medium and transferred to fresh medium after 2 weeks. After another 2 weeks, plants were classified as wild-type (I), moderate (II), or severe (III) phenotypes (see Figure 1B). The plants within each class were pooled, and the auxin concentration was measured in five samples from collected leaves and apical regions as described (Edlund et al., 1995).

Fluorometric GUS Assays

For quantification of GUS activity in *proLTP1*#8≫*iaaM*#20 F1 plants, seeds were germinated on medium containing kanamycin and PPT. Resistant seedlings were transferred to soil after 2 weeks, and after another 2 weeks, GUS activity was quantified in triplicate in two parallel protein extracts from the aboveground portion of the pooled plants of three defined classes (see above and Figure 1B) according to Jefferson et al. (1987).

Phenotypic Analysis and Histochemistry

Upon crossing, embryo phenotypes and GUS activity were analyzed by differential interference contrast microscopy in cleared ovules as described (Weijers et al., 2001). Siliques in which the majority of embryos were younger than the transition stage were abandoned from the analysis. Consistently, no obvious phenotypes were observed at preglobular stages.

Microscopy and Photography

Embryos were viewed on a Zeiss Axioplan II microscope equipped with differential interference contrast optics. Images were acquired in Adobe Photoshop using a Sony DKC5000 digital camera. Seedlings were photographed using a stereomicroscope equipped with a Sony DKC5000 digital camera. All image compositions and contrast enhancements were performed using Adobe Photoshop 6.0 and Adobe Illustrator 10.

ACKNOWLEDGMENTS

D.W. would like to thank Gerd Jürgens for enabling him to finish this work in his laboratory. We want to acknowledge Jan-Piet van Hamburg, Quirien Boone, Pierre-Jean Dublé, Nick Wierckx, Ab Quint, and Erwin van Rijn for excellent technical assistance, Enrico Scarpella, Bert van der Zaal, Rene Benjamins, and Niko Geldner for stimulating discussions, Harry Klee for plasmid pMON690, Jim Haseloff for making available the GAL4/*UAS* system and GAL4-enhancer trap lines, the Nottingham Arabidopsis Stock Centre for seed stocks, and Gerd Jürgens for helpful comments on the manuscript. This work was funded through grants from The Netherlands Organization for Scientific Research (D.W.), the European Molecular Biology Organization (ALTF582-2001 to D.W.), and the Volkswagenstiftung (M.S. and J.F.).

Received May 27, 2005; revised May 27, 2005; accepted June 25, 2005; published July 29, 2005.

REFERENCES

Aida, M., Vernoux, T., Furutani, M., Traas J., and Tasaka, M. (2002). Roles of PIN-FORMED1 and MONOPTEROS in pattern formation of the apical region of the Arabidopsis embryo. Development **129,** 3965–3974.

Barker, R.F., Idler, K.B., Thompson, D.V., and Kemp, J.D. (1983). Nucleotide sequence of the T-DNA region of the *Agrobacterium tumefaciens* octopine T1 plasmid pTi15955. Plant Mol. Biol. **2,** 335–350.

Blilou, I., Xu, J., Wildwater, M., Willemsen, V., Paponov, I., Friml, J., Heidstra, R., Aida, M., Palme, K., and Scheres, B. (2005). The PIN auxin efflux facilitator network controls growth and patterning in *Arabidopsis* roots. Nature **433,** 39–44.

Boisnard-Lorig, C., Colon-Carmona, A., Bauch, M., Hodge, S., Doerner, P., Bancharel, E., Dumas, C., Haseloff, J., and Berger, F. (2001). Dynamic analyses of the expression of the HISTONE:YFP fusion protein in *Arabidopsis* show that syncytial endosperm is divided in mitotic domains. Plant Cell **13,** 495–509.

Edlund, A., Eklöf, S., Sundberg, B., Moritz, T., and Sandberg, G. (1995). A microscale technique for gas chromatography-mass spectrometry measurements of pictogram amounts of indole-3-acetic acid in plant tissues. Plant Physiol. **108,** 1043–1047.

Friml, J. (2003). Auxin transport—Shaping the plant. Curr. Opin. Plant Biol. **6,** 7–12.

Friml, J., Benkova, E., Blilou, I., Wisniewska, J., Hamann, T., Ljung, K., Woody, S., Sandberg, G., Scheres, B., Jürgens, G., and Palme, K. (2002). AtPIN4 mediates sink-driven auxin gradients and root patterning in Arabidopsis. Cell **108,** 661–673.

Friml, J., Vieten, A., Sauer, M., Weijers, D., Schwarz, H., Hamann, T., Offringa, R., and Jürgens, G. (2003). Efflux-dependent auxin gradients establish the apical-basal axis of *Arabidopsis.* Nature **426,** 147–153.

Gray, W.M., Ostin, A., Sandberg, G., Romano, C.P., and Estelle, M. (1998). High temperature promotes auxin-mediated hypocotyl elongation in *Arabidopsis.* Proc. Natl. Acad. Sci. USA **95,** 7197–7202.

Hadfi, K., Speth, V., and Neuhaus, G. (1998). Auxin-induced developmental patterns in *Brassica juncea* embryos. Development **125,** 879–887.

Hamann, T., Benkova, E., Bäurle, I., Kientz, M., and Jürgens, G. (2002). The *Arabidopsis BODENLOS* gene encodes an auxin response protein inhibiting MONOPTEROS-mediated embryo patterning. Genes Dev. **16,** 1610–1615.

Hardtke, C.S., and Berleth, T. (1998). The *Arabidopsis* gene *MONOPTEROS* encodes a transcription factor mediating embryo axis formation and vascular development. EMBO J. **17,** 1405–1411.

Jefferson, R.A., Kavanagh, T.A., and Bevan, M.W. (1987). GUS fusions: β-Glucuronidase as a sensitive and versatile gene fusion marker in higher plants. EMBO J. **20,** 3901–3907.

Jiang, K., Meng, Y.L., and Feldman, L.J. (2003). Quiescent center formation in maize roots is associated with an auxin-regulated oxidizing environment. Development **130,** 1429–1438.

Johri, B.M., Ambegaokar, K.B., and Srivastava, P.S. (1992). Comparative Embryology of Angiosperms. (Heidelberg, Germany: Springer Verlag).

Jürgens, G., and Mayer, U. (1994). Arabidopsis. In Embryos, Color Atlas of Development, J.B.L. Bard, ed (London: Wolffe Publishing), pp. 7–22.

Klee, H.J., Horsch, R.B., Nichee, M.A., Hein, M.B., and Hoffmann, N.L. (1987). The effects of overproduction of two *Agrobacterium tumefaciens* T-DNA auxin biosynthetic gene products in transgenic petunia plants. Genes Dev. **1,** 86–96.

Liu, C.-M., Xu, Z., and Chua, N.-H. (1993). Auxin polar transport is essential for the establishment of bilateral symmetry during early plant embryogenesis. Plant Cell **5,** 621–630.

Long, J.A., Moan, E.I., Medford, J.I., and Barton, M.K. (1996). A member of the KNOTTED class of homeodomain proteins encoded by the *STM* gene of *Arabidopsis.* Nature **379,** 66–69.

Mansfield, S.G., and Briarty, L.G. (1991). Early embryogenesis in *Arabidopsis thaliana*. II. The developing embryo. Can. J. Bot. **69,** 461–467.

Romano, C.P., Hein, M.B., and Klee, H.J. (1991). Inactivation of auxin in tobacco transformed with the indoleacetic acid-lysine synthetase gene of *Pseudomonas savastanoi.* Genes Dev. **5,** 438–446.

Romano, C.P., Robson, P.R., Smith, H., Estelle, M., and Klee, H.J. (1995). Transgene-mediated auxin overproduction in *Arabidopsis*: Hypocotyl elongation phenotype and interactions with the *hy6-1* hypocotyl elongation and *axr1* auxin-resistant mutants. Plant Mol. Biol. **27,** 1071–1083.

Sabatini, S., Beis, D., Wolkenfelt, H., Murfett, J., Guilfoyle, T., Malamy, J., Benfey, P., Leyser, O., Bechtold, N., Weisbeek, P., and Scheres, B. (1999). An auxin-dependent distal organizer of pattern and polarity in the *Arabidopsis* root. Cell **99,** 463–472.

Sauer, M., and Friml, J. (2004). *In vitro* culture of *Arabidopsis* embryos within their ovules. Plant J. **40,** 835–843.

Schiavone, F.M., and Cooke, T.J. (1987). Unusual patterns of somatic embryogenesis in the domesticated carrot: Developmental effects of exogenous auxins and auxin transport inhibitors. Cell Differ. **21,** 53–62.

Sitbon, F., Ostin, A., Sundberg, B., Olsson, O., and Sandberg, G. (1992). Conjugation of indole-3-acetic acid (IAA) in wild-type and IAA-overproducing transgenic tobacco plants, and identification of the main conjugates by frit-fast atom bombardment liquid chromatography-mass spectrometry. Plant Physiol. **101,** 313–320.

Thoma, S., Hecht, U., Kippers, A., Botella, J., de Vries, S., and Somerville, C. (1994). Tissue-specific expression of a gene encoding a cell wall-localized lipid transfer protein from Arabidopsis. Plant Physiol. **105,** 35–45.

Ulmasov, T., Murfett, J., Hagen, G., and Guilfoyle, T.J. (1997). Aux/IAA proteins repress expression of reporter genes containing natural and highly active synthetic auxin response elements. Plant Cell **9,** 1963–1971.

Vroemen, C.W., Langeveld, S., Mayer, U., Ripper, G., Jürgens, G., van Kammen, A., and de Vries, S.C. (1996). Pattern formation in the *Arabidopsis* embryo revealed by position-specific lipid transfer protein gene expression. Plant Cell **8,** 783–791.

Weijers, D., Franke-van Dijk, M., Vencken, R.J., Quint, A., Hooykaas, P., and Offringa, R. (2001). An *Arabidopsis Minute*-like phenotype caused by a semi-dominant mutation in a *RIBOSOMAL PROTEIN S5* gene. Development **128,** 4289–4299.

Weijers, D., and Jürgens, G. (2005). Auxin and embryo axis formation: The ends in sight? Curr. Opin. Plant Biol. **8,** 32–37.

Weijers, D., van Hamburg, J.-P., van Rijn, E., Hooykaas, P.J.J., and Offringa, R. (2003). Diphteria toxin-mediated cell ablation reveals interregional communication during Arabidopsis seed development. Plant Physiol. **133,** 1882–1892.

Zhao, Y., Christensen, S.K., Fankhauser, C., Cashman, J.R., Cohen, J.D., Weigel, D., and Chory, J. (2001). A role for flavin monooxygenase-like enzymes in auxin biosynthesis. Science **291,** 306–309.